F. Kuwahara[1]
Department of Mechanical Engineering,
Shizuoka University,
3-5-1 Johoku, Naka-Ku,
Hamamatsu 432-8561, Japan
e-mail: tmfkuwa@ipc.shizuoka.ac.jp

C. Yang
Department of Mechanical Engineering,
Shizuoka University,
3-5-1 Johoku, Naka-Ku,
Hamamatsu 432-8561, Japan;
School of Energy and Power Engineering,
Huazhong University of Science and Technology,
Wuhan, Hubei 430074, P. R. China

K. Ando
Research Division,
Nitto Kogyo Corporation,
2201 Kanihara, Nagakute-Cho, Aichi-Gun,
Aichi 480-1189, Japan

A. Nakayama
Department of Mechanical Engineering,
Shizuoka University,
3-5-1 Johoku, Naka-Ku,
Hamamatsu 432-8561, Japan;
School of Civil Engineering and Architecture,
Wuhan Polytechnic University,
Wuhan, Hubei 430023, China

Exact Solutions for a Thermal Nonequilibrium Model of Fluid Saturated Porous Media Based on an Effective Porosity

An effective porosity concept has been introduced to account for the effects of tortuosity and thermal dispersion on the individual effective thermal conductivities of the solid and fluid phases in a fluid-saturated porous medium. Using this effective porosity concept, a thermal nonequilibrium model has been proposed to attack locally thermal nonequilibrium problems associated with convection within a fluid-saturated porous medium. Exact solutions are obtained, assuming a plug flow, for the two cases of thermally fully developed convective flows through a channel, namely, the case of isothermal hot and cold walls and the case of constant heat flux walls. These exact solutions for the cases of metal foam and air combination reveal that the local thermal equilibrium assumption may hold for the case of isothermal hot and cold walls, but may fail for the case of constant heat flux walls. [DOI: 10.1115/1.4004354]

Keywords: porous media, thermal nonequilibrium, aluminum, metal foam, conductivity

1 Introduction

There are two kinds of models to investigate thermal behavior of conduction and convection within a porous medium, namely, the so-called thermal equilibrium (single phase) model and thermal nonequilibrium (two phase) model. The local thermal equilibrium between the solid and fluid phases is assumed in the thermal equilibrium model, whereas no such assumption is assumed in the thermal nonequilibrium model. They are also called as one energy equation model and two energy equation model, respectively, since the thermal equilibrium model (which assumes that the temperatures of two phases are equal) deals only one energy equation, while the thermal nonequilibrium model (which allows the solid temperature to differ from the fluid temperature) retains two individual energy equations for the two phases.

One equation models based on the local thermal equilibrium assumption have been widely used in modeling transport phenomena in porous media, and have been proven to be quite effective for many cases of steady heat transfer without internal heat generation [1–4]. However, Quintard [5] and Quintard and Whitaker [6,7] pointed out that there are many physical situations in which the local thermal equilibrium assumption fails, and recommended use of a two energy equation model. The validity and assessment of the local thermal equilibrium assumptions were discussed by a substantial number of researchers, including Minkowycz et al. [8], Kim and Jang [9], Kiwana and Al-Nimr [10], Al-Mimr and Abu-Hijleh [11], Abu-Hijleh et al. [12], Khashan et al. [13], Khashan and Al-Nimr [14], and Haddad et al. [15].

There exit analytical investigations in which the exact solutions based on the local thermal equilibrium assumption have been examined by comparing the results against those based on a two equation model. Nakayama et al. [1] used the two energy equation model introduced by Hsu [16] and Hsu et al. [17], and obtained exact solutions for two fundamental steady heat transfer cases, namely, one-dimensional steady heat conduction in a porous slab with internal heat generation, and also thermally developing unidirectional flow through a semiinfinite porous medium. They pointed out that the thermal equilibrium assumption ceases to be valid even for certain steady thermal problems. Haddad et al. [15], on the other hand, treated free convection from a vertical plate embedded in a porous medium, and pointed out that the assumption of local thermal equilibrium may fail when the Rayleigh number is sufficiently high. Furthermore, Kuznetsov and Nield [18] investigated the onset of convection in a horizontal layer of a porous medium saturated by a nanofluid and reported that the effect of the local thermal equilibrium can be quite significant in certain circumstances. Kuznetsov [19,20] was also able to present perturbation solutions for thermal nonequilibrium problems associated with sensible heat storage packed beds.

Many investigators, who worked on two energy equation models, neglected the effects of tortuosity on the stagnant thermal conductivity, and simply evaluated the fluid phase thermal conductivity as a product of the porosity and its thermal conductivity, and likewise for the solid phase thermal conductivity. Such evaluations lead to significant errors in thermal conduction especially when the solid thermal conductivity is much higher than the fluid thermal conductivity, such as in the case of metal foams.

In this study, first, we shall propose an effective porosity concept to establish a two energy equation model, and derive a set of the volume averaged energy equations, which accounts for the tortuosity as well as the thermal dispersion. An aluminum foam and air combination is considered for illustration of effective thermal conductivities for the individual phases. Simple analytical expressions will be proposed to evaluate the thermal conductivities for the individual phases, which turn out to be significantly different from those based on simplified two energy equation models, used by most of previous investigators. Second, using this two energy

[1]Corresponding author.

Contributed by the Heat Transfer Division of ASME for publication in the JOURNAL OF HEAT TRANSFER. Manuscript received January 27, 2011; final manuscript received May 16, 2011; published online September 19, 2011. Assoc. Editor: Andrey Kuznetsov.

equation model, fully developed convective flows in a channel filled with an aluminum metal foam are considered to seek both fluid and solid temperature profiles across the channel. Exact solutions have been found for the case of isothermal walls as well as the case of constant wall heat flux. These exact solutions may be quite useful for the benchmark tests of numerical tools based on the thermal nonequilibrium assumption. Furthermore, the results show that the case of constant wall heat flux must be treated by using a thermal nonequilibrium model, since the fluid and solid phases within the channel never remain at thermal equilibrium. Exact and approximate solutions for another fundamental problem, namely, convection in a circular tube filled with a porous medium, may be found in an accompany paper [21], which provides all details of exhaustive mathematical manipulations.

2 Effective Porosity Concept

We shall consider the energy equation for the fluid phase and that for the solid matrix phase and integrate them over a local control volume, following the volume averaging theory [6,7,22,23]. The resulting volume averaged energy equations run as follows:

For the fluid phase

$$\varepsilon\rho_f c_{p_f}\frac{\partial\langle T\rangle^f}{\partial t}+\varepsilon\rho_f c_{p_f}\frac{\partial\langle u_j\rangle^f\langle T\rangle^f}{\partial x_j}=\frac{\partial}{\partial x_j}\left(\varepsilon k_f\frac{\partial\langle T\rangle^f}{\partial x_j}+\frac{k_f}{V}\int_{A_{\text{int}}}Tn_j dA-\rho_f c_{p_f}\varepsilon\langle\tilde{u}_j\tilde{T}\rangle^f\right)+\frac{1}{V}\int_{A_{\text{int}}}k_f\frac{\partial T}{\partial x_j}n_j dA \tag{1}$$

For the solid matrix phase

$$\rho_s c_s(1-\varepsilon)\frac{\partial\langle T\rangle^s}{\partial t}=\frac{\partial}{\partial x_j}\left((1-\varepsilon)k_s\frac{\partial\langle T\rangle^s}{\partial x_j}-\frac{k_s}{V}\int_{A_{\text{int}}}Tn_j dA\right)-\frac{1}{V}\int_{A_{\text{int}}}k_f\frac{\partial T}{\partial x_j}n_j dA \tag{2}$$

where the volume average of a certain variable ϕ in the fluid phase is defined as

$$\langle\phi\rangle^f\equiv\frac{1}{V_f}\int_{V_f}\phi dV$$

such that $\langle T\rangle^f$ is the intrinsic volume average of the fluid temperature, while $\langle T\rangle^s$ is the intrinsic volume average of the solid matrix temperature, where V_f is the volume space which the fluid phase occupies. The porosity $\varepsilon\equiv V_f/V$ is the volume fraction of the fluid space. The variable ϕ is decomposed into its intrinsic average and the spatial deviation from it

$$\phi=\langle\phi\rangle^f+\tilde{\phi}$$

Moreover, A_{int} is the local interfacial area between the fluid and solid phases, while n_i is the unit vector pointing outward from the fluid side to solid side. The continuity of both temperature and heat flux is imposed on the interface. Obviously, the parenthetical terms on the right hand-side of Eq. (1) denote the diffusive heat transfer, while the last term describes the interfacial heat transfer between the solid and fluid phases. Combining the foregoing two energy equations and noting the continuity of the temperature and heat flux at the interface, we obtain the single macroscopic equation as follows:

$$\frac{\partial\left(\varepsilon\rho_f c_{p_f}\langle T\rangle^f+(1-\varepsilon)\rho_s c_s\langle T\rangle^s\right)}{\partial t}+\varepsilon\rho_f c_{p_f}\frac{\partial\langle u_j\rangle^f\langle T\rangle^f}{\partial x_j}=\frac{\partial}{\partial x_j}\left(\varepsilon k_f\frac{\partial\langle T\rangle^f}{\partial x_j}+(1-\varepsilon)k_s\frac{\partial\langle T\rangle^s}{\partial x_j}+\frac{k_f-k_s}{V}\int_{A_{\text{int}}}Tn_j dA-\varepsilon\rho_f c_{p_f}\langle\tilde{u}_j\tilde{T}\rangle^f\right) \tag{3}$$

For the time being, let us assume $\partial\langle T\rangle^f/\partial x_j\cong\partial\langle T\rangle^s/\partial x_j\cong\partial\langle T\rangle/\partial x_j$. Then, the equation reduces to

$$\left(\varepsilon\rho_f c_{p_f}+(1-\varepsilon)\rho_s c_s\right)\frac{\partial\langle T\rangle}{\partial t}+\rho_f c_{p_f}\frac{\partial\langle u_j\rangle\langle T\rangle}{\partial x_j}=\frac{\partial}{\partial x_j}\left(\left(\varepsilon k_f+(1-\varepsilon)k_s\right)\frac{\partial\langle T\rangle}{\partial x_j}+\frac{k_f-k_s}{V}\int_{A_{\text{int}}}Tn_j dA-\varepsilon\rho_f c_{p_f}\langle\tilde{u}_j\tilde{T}\rangle^f\right) \tag{4}$$

where

$$\langle\phi\rangle\equiv\frac{1}{V}\int_V\phi dV \tag{5}$$

is the Darcian average of the variable ϕ such that $\langle u_j\rangle=\varepsilon\langle u_j\rangle^f$ is the Darcian velocity vector. From the foregoing Eq. (4), the macroscopic heat flux vector $q_i=(q_x,q_y,q_z)$ and its corresponding stagnant thermal conductivity k_{stag} may be defined as follows:

$$q_i=-k_{\text{stag}}\frac{\partial\langle T\rangle}{\partial x_i}+\varepsilon\rho_f c_{p_f}\langle\tilde{u}_i\tilde{T}\rangle^f=-\left(\varepsilon k_f+(1-\varepsilon)k_s\right)\frac{\partial\langle T\rangle}{\partial x_i}-\left(k_f-k_s\right)\frac{1}{V}\int_{A_{\text{int}}}Tn_i dA+\varepsilon\rho_f c_{p_f}\langle\tilde{u}_i\tilde{T}\rangle^f \tag{6}$$

The last term in the rightmost expression describes the thermal dispersion term, which describes an additional heat flux resulting from the hydrodynamic mixing due to the presence of obstacles, while the second term associated with the surface integral describes the effects of the tortuosity on the macroscopic heat flux. Note that the first term in the rightmost expression corresponds to the upper bound of the effective stagnant thermal conductivity based on the parallel model, namely, $\left(\varepsilon k_f+(1-\varepsilon)k_s\right)$. Thus, it is the tortuosity term (i.e., the second term) that adjusts the level of the effective stagnant thermal conductivity from its upper bound to a correct one. The effective porosity ε^* may be defined such that the stagnant thermal conductivity is given by

$$k_{\text{stag}}=\varepsilon^* k_f+(1-\varepsilon^*)k_s \tag{7a}$$

namely

$$\varepsilon^*=\frac{k_s-k_{\text{stag}}}{k_s-k_f}=\varepsilon+\frac{\varepsilon k_f+(1-\varepsilon)k_s-k_{\text{stag}}}{k_s-k_f} \tag{7b}$$

such that

$$(\varepsilon^*-\varepsilon)\frac{\partial\langle T\rangle}{\partial x_i}=\frac{1}{V}\int_{A_{\text{int}}}Tn_i dA \tag{8}$$

The stagnant thermal conductivity k_{stag} is given experimentally, or, it can be estimated using some empirical and theoretical expressions. We shall discuss such expressions shortly. Using the effective porosity ε^*, the energy Eqs. (1) and (2) may be rewritten concisely as follows:

For the fluid phase

$$\rho_f c_{p_f}\varepsilon\frac{\partial\langle T\rangle^f}{\partial t}+\rho_f c_{p_f}\frac{\partial\langle u_j\rangle\langle T\rangle^f}{\partial x_j}=\frac{\partial}{\partial x_j}\left(\varepsilon^* k_f\frac{\partial\langle T\rangle^f}{\partial x_j}+\varepsilon k_{dis_{jk}}\frac{\partial\langle T\rangle^f}{\partial x_k}\right)-h_v\left(\langle T\rangle^f-\langle T\rangle^s\right) \tag{9}$$

For the solid matrix phase

$$\rho_s c_s(1-\varepsilon)\frac{\partial\langle T\rangle^s}{\partial t}=\frac{\partial}{\partial x_j}\left((1-\varepsilon^*)k_s\frac{\partial\langle T\rangle^s}{\partial x_j}\right)-h_v\left(\langle T\rangle^s-\langle T\rangle^f\right) \tag{10}$$

where the thermal dispersion term is modeled according to the gradient diffusion hypothesis [24]

$$-\rho_f c_{p_f}\langle\tilde{u}_j\tilde{T}\rangle^f = k_{\mathrm{dis}_{kj}}\frac{\partial\langle T\rangle^f}{\partial x_k} \tag{11}$$

while the interfacial heat transfer between the solid and fluid phases is modeled using Newton's cooling law

$$\frac{1}{V}\int_{A_{\mathrm{int}}} k_f\frac{\partial T}{\partial x_j}n_j dA = h_v\left(\langle T\rangle^s - \langle T\rangle^f\right) \tag{12}$$

where h_v is the volumetric heat transfer coefficient.

3 Stagnant Thermal Conductivities of Metal Foams

Yang and Nakayama [25] proposed a general unit cell model based on the volume averaging theory and evaluated stagnant thermal conductivities of packed beds, screen wires, and metal foams, which show good agreement with available experimental data. The structure of metal foams of our interest is quite complex, since their cells are usually polyhedrons of many faces in which each face has a pentagon or hexagonal shape. Therefore, it may not be practical to describe all details of the structure accurately. Thus, Yang and Nakayama [25] appealed to a foam cell geometry idealization and applied their general unit model to high porosity metal foams. Faithfully following the volume average theory, they derived an analytical expression, which runs as

$$\frac{k_{\mathrm{stag}}}{k_f} = \sigma\xi^2 + (1-\xi)^2 + \frac{2\xi(1-\xi)\sigma}{\xi+\sigma(1-\xi)} \tag{13}$$

where

$$\varepsilon = 1 - 3\xi^2 + 2\xi^3 \tag{14}$$

Equation (13) is a function of only two parameters, namely, the thermal conductivity ratio $\sigma = k_s/k_f$ and the porosity ε. It turns out to be mathematically identical to the formulas obtained by Hsu et al. [17] and Paek et al. [26]. Paek et al. used Dul'nev's model [27], which transforms an open-cell porous medium consisting of polygonal foam geometry to an equivalent cubic cell model.

For the case of high porosity (i.e., $\xi \ll 1$) and high thermal conductivity ratio such as in metal foam and air combinations of our interest, we typically have $\sigma = 8200$ and $\varepsilon = 0.95$. Thus, the condition $\sigma \gg 3/(1-\varepsilon)$ is satisfied. For such cases, Eq. (13) along with Eq. (14) can further be simplified as

$$\frac{k_{\mathrm{stag}}}{k_f} = \sigma\frac{1-\varepsilon}{3} \tag{15}$$

which turns out to be identical to the expression derived by Krishnan et al. [28]. They used the Lemlich theory [29], in which it is assumed that the conduction for the case of polyhedral foams of high porosity occurs only through the ligament of solid foams along its axis, and not through its periphery.

Calmidi and Mahajan [30,31] approximated a complex foam structure, introducing a hexagonal structure. In this way, they were able to obtain an expression for the effective stagnant thermal conductivity based on a one-dimensional heat conduction concept. Their expression, which is a function of three geometrical parameters in addition to the thermal conductivity ratio $\sigma = k_s/k_f$, agrees fairly well with available experimental data, although it is limited to their particular fibrous metal foam structure. Calmidi and Mahajan [30] carried out a series of measurements using various metal foams. Air and water were used to measure the effective thermal conductivity of metal foams. Based on the experimental data collected, they proposed the following empirical formula:

$$\frac{k_{\mathrm{stag}}}{k_f} = \varepsilon + 0.19(1-\varepsilon)^{0.763}\sigma \tag{16}$$

Another set of experimental data were provided by Bhattacharya et al. [32] for a wider range of the thermal conductivity ratio, using foams of reticulated vitreous carbon (RVC) with air and water as the fluid media. Their empirical correlation, which blends the effective thermal conductivities in series and parallel arrangement of the fluid and solid phases, is given as follows:

$$\frac{k_{\mathrm{stag}}}{k_f} = 0.35\{\varepsilon + (1-\varepsilon)\sigma\} + \frac{0.65}{\left(\varepsilon + \dfrac{1-\varepsilon}{\sigma}\right)} \tag{17}$$

Singh and Kasana [33] collected available experimental data on the thermal conductivities of metal foams and fitted them to determine the most appropriate expression for their exponent F as follows:

$$\frac{k_{\mathrm{stag}}}{k_f} = \{\varepsilon + (1-\varepsilon)\sigma\}^F\left(\varepsilon + \frac{1-\varepsilon}{\sigma}\right)^{-(1-F)} \tag{18}$$

where

$$F = 0.3031 + 0.0623\ln(\varepsilon\sigma) \tag{19}$$

All the forgoing analytical and empirical expressions are plotted together with some available experimental data for air as the fluid medium in Fig. 1. (Note that Eq. (13) is indicated by a solid line in the figure.) These analytical and empirical expressions indicate reasonably good agreement with the available experimental data collected by Calmidi and Mahajan [30]. It can be seen that, for metal foam and air combinations, the simple expression (15) is sufficiently accurate to correlate their stagnant thermal conductivities in a wide range of the porosity.

Calmidi and Mahajan [31] suggested using $k_{\mathrm{stag}}\big|_{k_s=0}$ for the fluid phase conductivity and $k_{\mathrm{stag}}\big|_{k_f=0}$ for the solid phase conductivity for their two energy equation model. However, the foregoing Eqs. (9) and (10), which account for both tortuosity and dispersion, reveal that the correct stagnant thermal conductivities for the fluid phase and solid phase are given by

$$\varepsilon^* k_f = \frac{\sigma - \left(k_{\mathrm{stag}}/k_f\right)}{\sigma - 1}k_f \tag{20a}$$

and

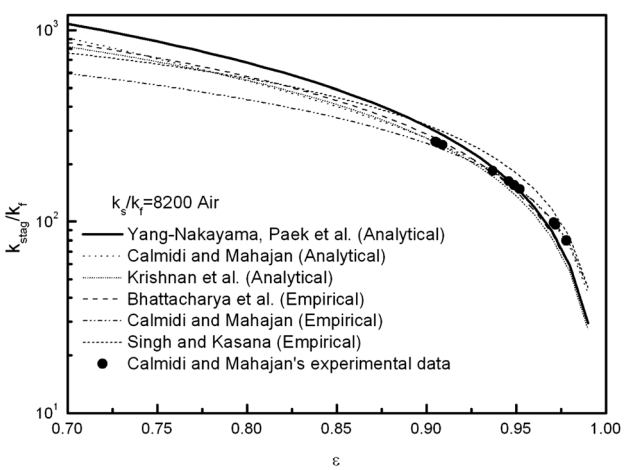

Fig. 1 Various expressions for stagnant thermal conductivity of aluminum metal foam saturated with air

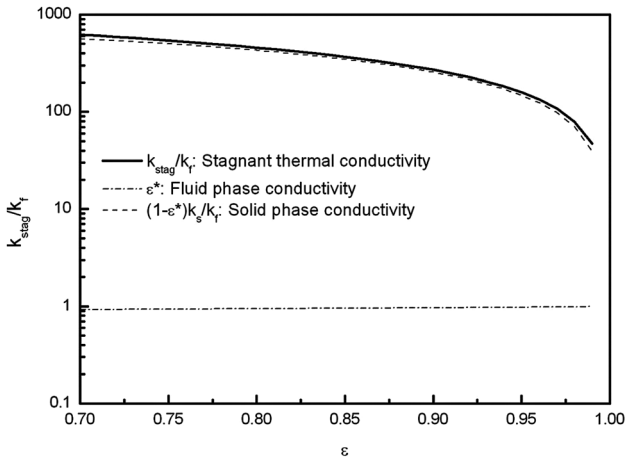

Fig. 2 Thermal conductivities of the fluid and solid phases in aluminum foam and air combination

$$(1-\varepsilon^*)k_s = \frac{(k_{\text{stag}}/k_f)-1}{\sigma-1}k_s \tag{20b}$$

respectively.

In Fig. 2, the thermal conductivities for the fluid phase and solid phase are plotted for the case of aluminum foam and air combination, faithfully following the foregoing Eqs. (20*a*) and (20*b*) along with Calmidi and Mahajan's empirical formula (16) for k_{stag}.

It is interesting to note that the aluminum phase stagnant conductivity is fairly close to the total stagnant thermal conductivity itself, $k_{\text{stag}} \cong (1-\varepsilon^*)k_s$. This is due to the fact that the aluminum thermal conductivity is so much higher than the air thermal conductivity that $\sigma \gg 3/(1-\varepsilon)$ and the simple expression (15) holds such that

$$\varepsilon^* = \frac{k_s - k_{\text{stag}}}{k_s - k_f} \cong \frac{k_s - \dfrac{1-\varepsilon}{3}k_s}{k_s - k_f} \cong \frac{2+\varepsilon}{3} \tag{21}$$

Thus, the individual thermal conductivities for the air phase and aluminum phase are given by

$$\varepsilon^* k_f = \frac{2+\varepsilon}{3}k_f \tag{22a}$$

and

$$(1-\varepsilon^*)k_s = \frac{1-\varepsilon}{3}k_s \cong k_{\text{stag}} \tag{22b}$$

respectively. For the metal foam and air combinations, the foregoing approximate Eqs. (22*a*) and (22*b*) may be used for the individual phase energy equations. It should be noted that these results substantially differ from the conventional expressions for the fluid phase and solid phase conductivities used by many previous investigators, namely, εk_f and $(1-\varepsilon)k_s$.

4 Convective Heat Transfer Through a Channel Filled With a Metal Foam Bounded by Isothermal Hot and Cold Walls

Prior to its application to the cases of metal foam and air combinations, the set of the Eqs. (9) and (10) based on the effective porosity concept was used to consider one of the fundamental packed bed problems, namely, thermally developing unidirectional flow through a semiinfinite packed bed, which was treated by Nakayama et al. [1] using somewhat more complex two equation model introduced by Hsu et al. [17]. The results based on the present model are found to agree well with those reported by Nakayama et al. [1], which substantiates the validity of the present model based on the effective porosity concept.

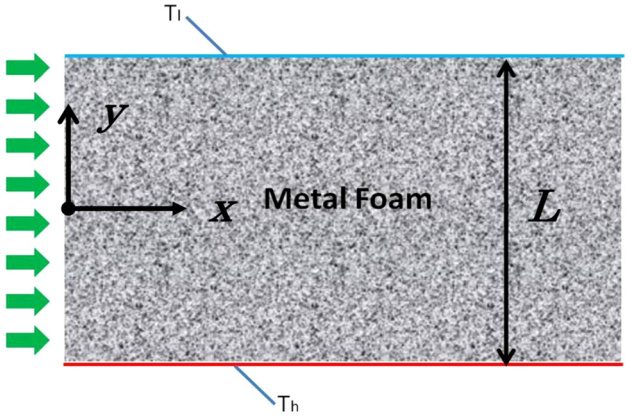

Fig. 3 Heat transfer in a channel filled with a metal foam bounded by isothermal walls

Now, we shall seek possible exact solutions for convective heat transfer in a channel filled with metal foams, using our thermal nonequilibrium model. For this first case, as shown in Fig. 3, the air is flowing through an infinitely long channel of height L filled with a metal foam. The lower bounding wall is isothermally heated to a constant temperature T_h while the upper wall is isothermally cooled to a constant temperature T_l. As pointed out by Dukhan et al. [34] and Nakayama et al. [35], the Darcian velocity shows its dependence on the transverse direction only in a small region very close to the walls. Therefore, we may neglect the boundary term (i.e., Brinkman term) and use the plug-flow approximation. Under this approximation, sufficiently away from the entrance, the energy Eqs. (9) and (10) for the individual phases reduce to the following ordinary differential equations

For the fluid phase

$$\left(\varepsilon^* k_f + \varepsilon k_{\text{dis}_{yy}}\right)\frac{d^2\langle T\rangle^f}{dy^2} - h_v\left(\langle T\rangle^f - \langle T\rangle^s\right) = 0 \tag{23}$$

For the solid phase

$$(1-\varepsilon^*)k_s\frac{d^2\langle T\rangle^s}{dy^2} - h_v\left(\langle T\rangle^s - \langle T\rangle^f\right) = 0 \tag{24}$$

The boundary conditions for the individual phase temperatures are given by

$$y = -L/2 : \langle T\rangle^s = T_h, \quad \langle T\rangle^f = T_h - \Delta T \tag{25a}$$

$$y = L/2 : \langle T\rangle^s = T_l, \quad \langle T\rangle^f = T_l + \Delta T \tag{25b}$$

Note that both solid and fluid phase temperatures must be prescribed at the upper and lower walls. The same temperature difference ΔT is set at the upper and lower walls for both temperature profiles to become symmetry about the center plane of the channel, which then guarantees the uniform heat flux across the channel. Adding these two energy equations, one obtains the total heat flux directing upward from the lower wall to the upper wall

$$q_w = -\left(\varepsilon^* k_f + \varepsilon k_{\text{dis}_{yy}}\right)\frac{d\langle T\rangle^f}{dy} - (1-\varepsilon^*)k_s\frac{d\langle T\rangle^s}{dy} = \text{const.} \tag{26}$$

which can be integrated to give the relationship between the solid and fluid phase temperatures as

$$\left(\varepsilon^* k_f + \varepsilon k_{\mathrm{dis}_{yy}}\right)\left(\langle T\rangle^f - (T_h - \Delta T)\right) + (1-\varepsilon^*)k_s(\langle T\rangle^s - T_h) = -q_w\left(y + \frac{L}{2}\right) \tag{27}$$

For given wall temperatures, the wall heat flux q_w can easily be evaluated from

$$q_w = \left(k_{\mathrm{stag}} + \varepsilon k_{\mathrm{dis}_{yy}}\right)\frac{T_h - T_l}{L} - 2\left(\varepsilon^* k_f + \varepsilon k_{\mathrm{dis}_{yy}}\right)\frac{\Delta T}{L} \tag{28}$$

Substituting the foregoing relationship into Eq. (24) to eliminate $\langle T\rangle^f$ in favor of $\langle T\rangle^s$, we obtain the following second order ordinary differential equation with respect to $\langle T\rangle^s$

$$(1-\varepsilon^*)k_s\frac{d^2\langle T\rangle^s}{dy^2} - \frac{k_{\mathrm{stag}} + \varepsilon k_{\mathrm{dis}_{yy}}}{\varepsilon^* k_f + \varepsilon k_{\mathrm{dis}_{yy}}}h_v\left(\langle T\rangle^s - \frac{T_h + T_l}{2}\right) = \frac{q_w}{\varepsilon^* k_f + \varepsilon k_{\mathrm{dis}_{yy}}}h_v y \tag{29}$$

which can be solved as

$$\frac{\langle T\rangle^s - \frac{T_h + T_l}{2}}{T_h - T_l} = -\frac{y}{L} + \frac{\varepsilon^* k_f + \varepsilon k_{\mathrm{dis}_{yy}}}{k_{\mathrm{stag}} + \varepsilon k_{\mathrm{dis}_{yy}}}\left(\frac{\Delta T}{T_h - T_l}\right) \times \left(\left(\frac{y}{L/2}\right) - \frac{\sinh(\lambda y)}{\sinh\left(\lambda\frac{L}{2}\right)}\right) \tag{30a}$$

and the relationship Eq. (27) between the solid and fluid phase temperatures gives

$$\frac{\langle T\rangle^f - \frac{T_h + T_l}{2}}{T_h - T_l} = -\frac{y}{L} + \frac{\varepsilon^* k_f + \varepsilon k_{\mathrm{dis}_{yy}}}{k_{\mathrm{stag}} + \varepsilon k_{\mathrm{dis}_{yy}}}\left(\frac{\Delta T}{T_h - T_l}\right) \times \left(\left(\frac{y}{L/2}\right) + \frac{(1-\varepsilon^*)k_s}{\varepsilon^* k_f + \varepsilon k_{\mathrm{dis}_{yy}}}\frac{\sinh(\lambda y)}{\sinh\left(\lambda\frac{L}{2}\right)}\right) \tag{30b}$$

where

$$\lambda = \sqrt{\frac{\left(k_{\mathrm{stag}} + \varepsilon k_{\mathrm{dis}_{yy}}\right)h_v}{\left(\varepsilon^* k_f + \varepsilon k_{\mathrm{dis}_{yy}}\right)(1-\varepsilon^*)k_s}} \tag{31a}$$

The dimensionless temperature difference $\Delta T/(T_h - T_l)$ indicates the degree of thermal nonequilibrium. For the case of aluminum foam and air combination, λ can be approximated using Eqs. (15) and (21) by

$$\lambda d_m = \sqrt{\frac{\frac{1-\varepsilon}{3}\sigma + \varepsilon\frac{k_{\mathrm{dis}_{yy}}}{k_f}}{\left(\frac{2+\varepsilon}{3} + \varepsilon\frac{k_{\mathrm{dis}_{yy}}}{k_f}\right)\frac{1-\varepsilon}{3}\sigma}\left(\frac{h_v d_m^2}{k_f}\right)} \tag{31b}$$

Calmidi and Mahajan [30,31] examined experimental data available for the case of aluminum foam and air combination, and proposed the empirical correlations for the volumetric heat transfer coefficient and the dispersion coefficient as follows:

$$Nu_v = \frac{h_v d_m^2}{k_f} = 8.72(1-\varepsilon)^{1/4}\left(\frac{1 - e^{-(1-\varepsilon)/0.04}}{\varepsilon}\right)^{1/2}\left(\frac{u_D d_m}{\nu}\right)^{1/2} Pr^{0.37} \tag{32}$$

$$\frac{\varepsilon k_{\mathrm{dis}_{yy}}}{k_f} = 0.06\left(\frac{\rho_f c_{p_f} u_D\sqrt{K}}{k_f}\right) \tag{33}$$

where u_D is the Darcian velocity, and the permeability is given by the following empirical correlation [31]:

$$K/d_m^2 = 0.00073(1-\varepsilon)^{-0.224}\left(\frac{1.18}{1 - e^{-(1-\varepsilon)/0.04}}\sqrt{\frac{1-\varepsilon}{3\pi}}\right)^{-1.11} \tag{34}$$

where d_m is the pore diameter. The temperature profiles for both phases for the case of $\sigma = 8200$, $\varepsilon = 0.95$, $\rho_f c_{p_f} u_D L/k_f = 5000$, $d_m/L = 0.1$, $K/d_m^2 = 0.015$, and $\Delta T/(T_h - T_l) = 0.5/20 = 0.025$ are illustrated in Fig. 4 for convective uniform flow through a channel.

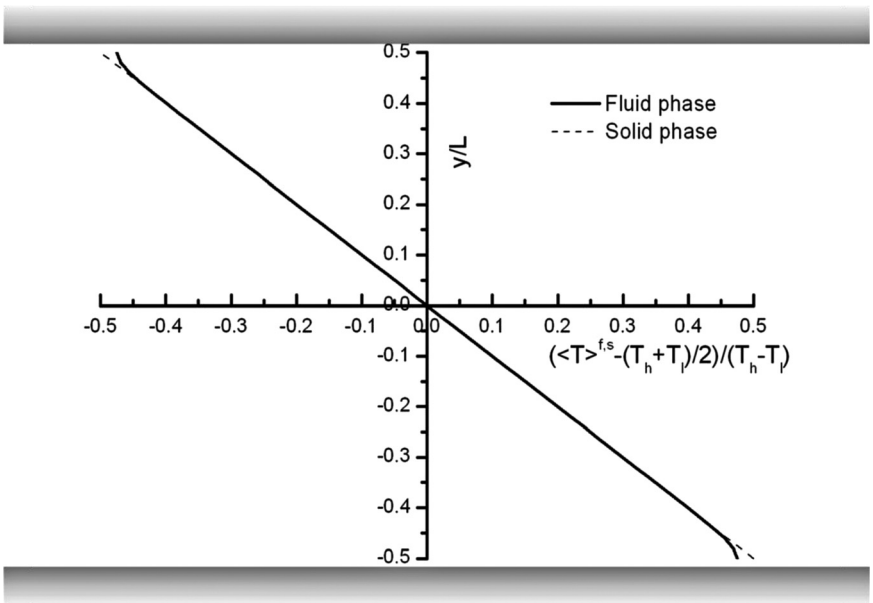

Fig. 4 Fluid and solid temperature profiles in a metal foam channel with isothermal walls

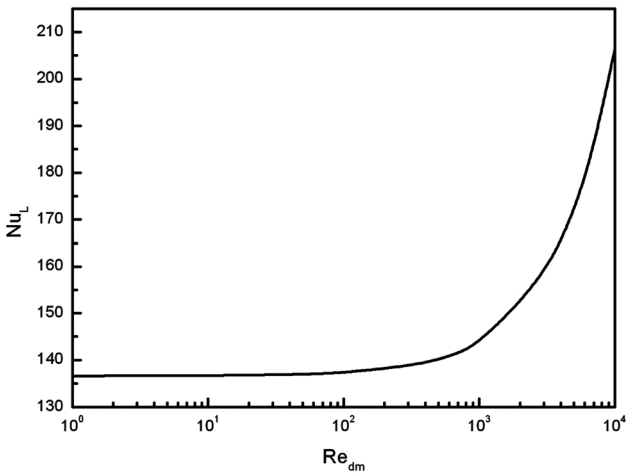

Fig. 5 The Nusselt number for a metal foam channel with isothermal walls

The temperature difference between the phases is appreciable only in a thin layer very close to the walls. After carrying out a series of computations based on Eqs. (30*a*) and (30*b*) for wide ranges of the parameters, it has been confirmed that an increase in $\Delta T/(T_h - T_l)$ does not affect the thickness of the layer much. The two phases are found nearly at thermal equilibrium over most of the channel cross-section, justifying the local thermal equilibrium assumption for this case of isothermal walls.

According to Eq. (28), the Nusselt number is given by

$$Nu_L = \frac{q_w L}{(T_h - T_l)k_f} = \frac{1-\varepsilon}{3}\sigma + \varepsilon\frac{k_{\mathrm{dis}_{yy}}}{k_f} - 2\left(\frac{2+\varepsilon}{3} + \varepsilon\frac{k_{\mathrm{dis}_{yy}}}{k_f}\right)\left(\frac{\Delta T}{T_h - T_l}\right) \tag{35}$$

As illustrated in Fig. 5, the Nusselt number increases with the Reynolds number $Re_{d_m} = u_D d_m/\nu$, since the thermal dispersion increases with the Reynolds number. However, Eq. (35) indicates that a high degree of thermal nonequilibrium results in diminishing the Nusselt number.

5 Convective Heat Transfer Through a Channel Filled With a Metal Foam Bounded by Constant Heat Flux Walls

In this second case, as shown in Fig. 6, both upper and lower bounding walls are heated by constant wall heat flux q_w. Thus, the boundary condition is given by

$$q_w = \left(\varepsilon^* k_f + \varepsilon k_{\mathrm{dis}_{yy}}\right)\left.\frac{\partial\langle T\rangle^f}{\partial y}\right|_{y=\pm L/2} + (1-\varepsilon^*)k_s\left.\frac{\partial\langle T\rangle^s}{\partial y}\right|_{y=\pm L/2} \tag{36}$$

The energy Eqs. (9) and (10) for the individual phases for this case may be written as

For the fluid phase

$$\rho_f c_{p_f} u_D \frac{\partial\langle T\rangle^f}{\partial x} = \left(\varepsilon^* k_f + \varepsilon k_{\mathrm{dis}_{yy}}\right)\frac{\partial^2\langle T\rangle^f}{\partial y^2} - h_v\left(\langle T\rangle^f - \langle T\rangle^s\right) \tag{37}$$

For the solid phase

$$(1-\varepsilon^*)k_s\frac{\partial^2\langle T\rangle^s}{\partial y^2} - h_v\left(\langle T\rangle^s - \langle T\rangle^f\right) = 0 \tag{38}$$

which may be added to give

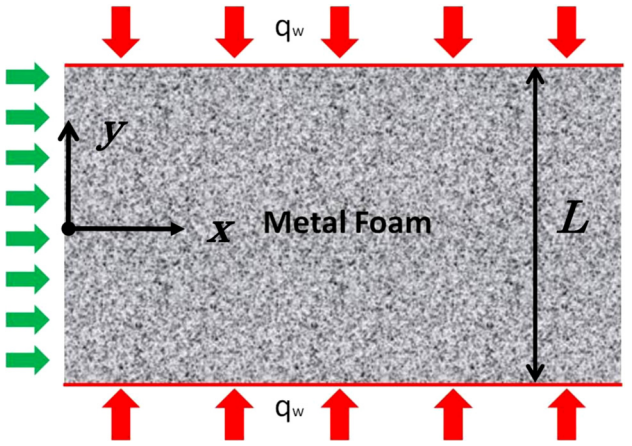

Fig. 6 Heat transfer in a channel filled with a metal foam bounded by constant heat flux walls

$$\rho_f c_{p_f} u_D \frac{\partial\langle T\rangle^f}{\partial x} = \frac{\partial}{\partial y}\left(\left(\varepsilon^* k_f + \varepsilon k_{\mathrm{dis}_{yy}}\right)\frac{\partial\langle T\rangle^f}{\partial y} + (1-\varepsilon^*)k_s\frac{\partial\langle T\rangle^s}{\partial y}\right) \tag{39}$$

Upon integrating the foregoing Eq. (39) over the channel with the boundary condition given by Eq. (36), the energy balance readily gives us

$$\rho_f c_{p_f} u_D L\frac{d\langle T\rangle_B^f}{dx} = 2q_w$$

Hence,

$$\frac{d\langle T\rangle_B^f}{dx} = \frac{\partial\langle T\rangle^f}{\partial x} = \frac{\partial\langle T\rangle^s}{\partial x} = \frac{2q_w}{\rho_f c_{p_f} u_D L} \tag{40}$$

for this case of constant heat flux, which can be substituted into Eq. (39) to give

$$\frac{\partial}{\partial y}\left(\left(\varepsilon^* k_f + \varepsilon k_{\mathrm{dis}_{yy}}\right)\frac{\partial\langle T\rangle^f}{\partial y} + (1-\varepsilon^*)k_s\frac{\partial\langle T\rangle^s}{\partial y}\right) = 2\frac{q_w}{L}$$

which may be integrated as

$$\left(\varepsilon^* k_f + \varepsilon k_{\mathrm{dis}_{yy}}\right)\frac{\partial\langle T\rangle^f}{\partial y} + (1-\varepsilon^*)k_s\frac{\partial\langle T\rangle^s}{\partial y} = 2\frac{q_w}{L}y$$

where the symmetry condition at $y=0$ is exploited. The equation can further be integrated as

$$\left(\varepsilon^* k_f + \varepsilon k_{\mathrm{dis}_{yy}}\right)\left((T_w - \Delta T) - \langle T\rangle^f\right) + (1-\varepsilon^*)k_s(T_w - \langle T\rangle^s) = \frac{q_w}{L}\left(\left(\frac{L}{2}\right)^2 - y^2\right) \tag{41}$$

where $\langle T\rangle^s|_{y=\pm L/2} = T_w$ and $\langle T\rangle^f|_{y=\pm L/2} = T_w - \Delta T$. The degree of thermal nonequilibrium, $\Delta T = (\langle T\rangle^s - \langle T\rangle^f)|_{y=\pm L/2}$, must be prescribed. The foregoing relationship (41) between the solid and fluid temperatures is substituted into Eq. (38) to obtain the following ordinary differential equation in terms of $(\langle T\rangle^s - T_w)$, which is a function of y alone, as

$$(1-\varepsilon^*)k_s\frac{d^2(\langle T\rangle^s - T_w)}{dy^2} - \frac{k_{\mathrm{stag}} + \varepsilon k_{\mathrm{dis}_{yy}}}{\varepsilon^* k_f + \varepsilon k_{\mathrm{dis}_{yy}}}h_v(\langle T\rangle^s - T_w) = -\frac{h_v q_w}{\left(\varepsilon^* k_f + \varepsilon k_{\mathrm{dis}_{yy}}\right)L}y^2 + h_v\left(\Delta T + \frac{q_w L}{4\left(\varepsilon^* k_f + \varepsilon k_{\mathrm{dis}_{yy}}\right)}\right) \tag{42}$$

This ordinary differential equation, after considerable manipulations, yields

$$\frac{\langle T\rangle^s - T_w}{Lq_w/\left(k_{\text{stag}}+\varepsilon k_{\text{dis}_{yy}}\right)} = \frac{1}{4}\left(\left(\frac{y}{L/2}\right)^2 - 1 + \frac{8}{(\lambda L)^2}\left(1-\frac{\cosh(\lambda y)}{\cosh(\lambda L/2)}\right)\right) - \frac{\varepsilon^* k_f + \varepsilon k_{\text{dis}_{yy}}}{k_{\text{stag}}+\varepsilon k_{\text{dis}_{yy}}}\left(1-\frac{\cosh(\lambda y)}{\cosh(\lambda L/2)}\right) \times \left(\frac{\Delta T}{Lq_w/\left(k_{\text{stag}}+\varepsilon k_{\text{dis}_{yy}}\right)}\right) \tag{43a}$$

and

$$\frac{\langle T\rangle^f - T_w}{Lq_w/\left(k_{\text{stag}}+\varepsilon k_{\text{dis}_{yy}}\right)} = \frac{1}{4}\left(\left(\frac{y}{L/2}\right)^2 - 1 - \frac{(1-\varepsilon^*)k_s}{\varepsilon^* k_f + \varepsilon k_{\text{dis}_{yy}}}\frac{8}{(\lambda L)^2}\left(1-\frac{\cosh(\lambda y)}{\cosh(\lambda L/2)}\right)\right) + \left(\frac{(1-\varepsilon^*)k_s}{k_{\text{stag}}+\varepsilon k_{\text{dis}_{yy}}}\left(1-\frac{\cosh(\lambda y)}{\cosh(\lambda L/2)}\right) - 1\right)\left(\frac{\Delta T}{Lq_w/\left(k_{\text{stag}}+\varepsilon k_{\text{dis}_{yy}}\right)}\right) \tag{43b}$$

where λ is as already defined by Eq. (31*a*). Let us consider the two asymptotic conditions for the degree of thermal nonequilibrium, ΔT, namely, the local thermal equilibrium condition at the wall, i.e. $\Delta T = 0$, and the local uniform heat flux condition at the wall, as given by (Fig. 6)

$$q_w = \frac{\varepsilon^* k_f + \varepsilon k_{\text{dis}_{yy}}}{\varepsilon}\frac{\partial\langle T\rangle^f}{\partial y}\bigg|_{y=\pm L/2} = \frac{1-\varepsilon^*}{1-\varepsilon}k_s\frac{\partial\langle T\rangle^s}{\partial y}\bigg|_{y=\pm L/2}$$

which gives

$$\frac{\Delta T}{Lq_w/\left(k_{\text{stag}}+\varepsilon k_{\text{dis}_{yy}}\right)} = \frac{\dfrac{1-\varepsilon}{1-\varepsilon^*}\dfrac{k_{\text{stag}}+\varepsilon k_{\text{dis}_{yy}}}{k_s} + \dfrac{\tanh(\lambda L/2)}{(\lambda L/2)} - 1}{\dfrac{\varepsilon^* k_f + \varepsilon k_{\text{dis}_{yy}}}{k_{\text{stag}}+\varepsilon k_{\text{dis}_{yy}}}(\lambda L)\tanh(\lambda L/2)} \tag{44}$$

The fluid and solid temperature profiles across the upper half channel are illustrated for the aluminum foam and air combination, $\sigma = 8200$, $\varepsilon = 0.95$, $\rho_f c_{p_f} u_D L/k_f = 5000$ $d_m/L = 0.1$, and $K/d_m^2 =$ 0.015 in Figs. 7(*a*) and 7(*b*) for these two asymptotic cases, namely, the local thermal equilibrium wall case and the local uniform heat flux wall case, respectively. As before, Eqs. (32)–(34) are used to evaluate the volumetric heat transfer coefficient and the dispersion coefficient. It should be noted that the local uniform heat flux condition at the wall, as shown in Fig. 7(*b*), yields negative $\Delta T = (\langle T\rangle^s - \langle T\rangle^f)\big|_{y=\pm L/2}$, since, under such a wall condition, the fluid temperature gradient at the wall stays so high to generate the required heat flux, that the fluid temperature exceeds the solid temperature at the wall. However, this asymptotic condition appears to be unrealistic. The other asymptotic condition of local thermal equilibrium wall ($\Delta T = 0$), as illustrated in Fig. 7(*a*), may be much closer to reality for the case of base materials with sufficiently high thermal conductivity. Thus, the assumption of local thermal equilibrium wall ($\Delta T = 0$) may be used for practical estimations. As both figures clearly show that the solid temperature in the core region is always substantially higher than the fluid temperature for the case of channels with constant heat flux walls, irrespective of the degree of thermal nonequilibrium, ΔT. Therefore, the local thermal equilibrium assumption ceases to be valid for the case of constant heat flux walls.

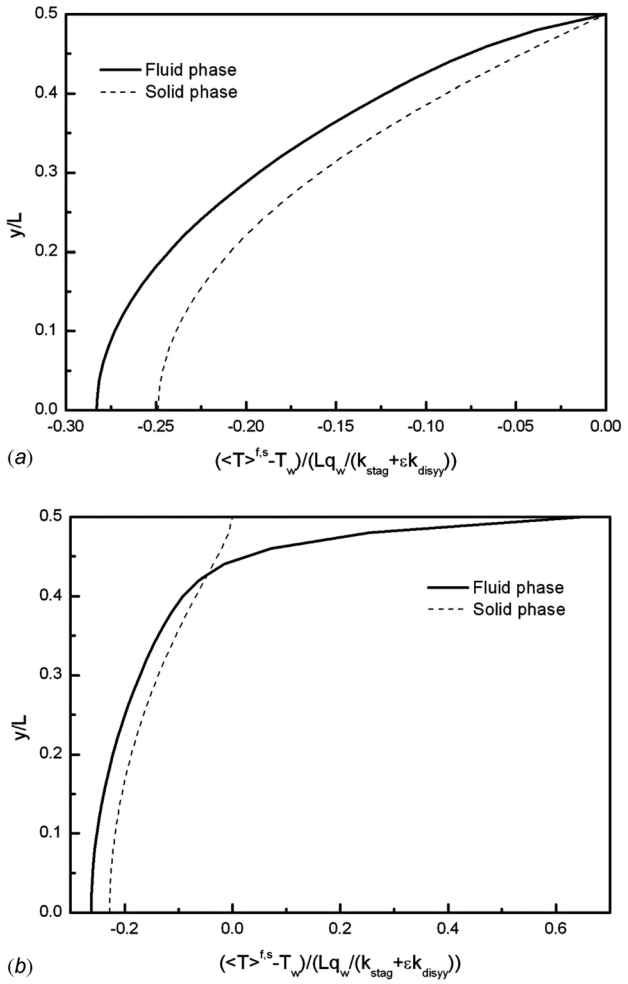

Fig. 7 Fluid and solid temperature profiles in a metal foam channel with constant heat flux: (*a*) local thermal equilibrium walls ($\Delta T = 0$) and (*b*) local uniform heat flux walls

Finally, the Nusselt number for the case of local thermal equilibrium at the wall ($\Delta T = 0$) is presented in Fig. 8, which

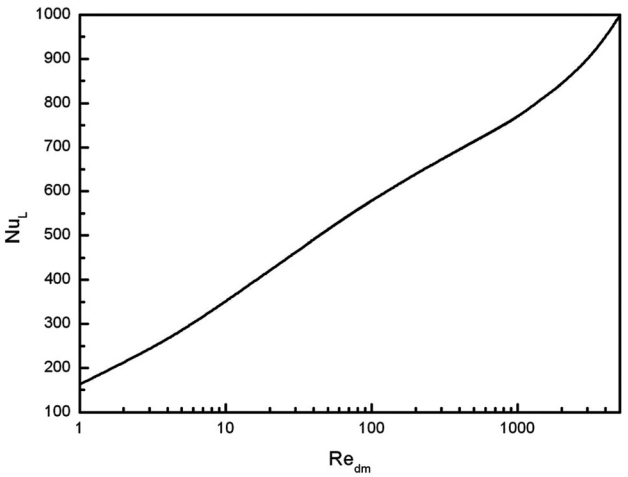

Fig. 8 The Nusselt number for a metal foam channel with constant heat flux walls

indicates monotonous increase in the Nusselt number with the Reynolds number.

$$Nu_L = \frac{q_w L}{\left(T_w - \langle T \rangle_B^f\right) k_f} = \frac{6\dfrac{k_{\text{stag}} + \varepsilon k_{\text{dis}_{yy}}}{k_f}}{1 + \dfrac{(1-\varepsilon^*)k_s}{\varepsilon^* k_f + \varepsilon k_{\text{dis}_{yy}}} \dfrac{12}{(\lambda L)^2}\left(1 - \dfrac{\tanh(\lambda L/2)}{(\lambda L/2)}\right)}$$
$$= \frac{6\left(\dfrac{1-\varepsilon}{3}\sigma + \dfrac{\varepsilon k_{\text{dis}_{yy}}}{k_f}\right)}{1 + \dfrac{(1-\varepsilon)\sigma}{\left(\dfrac{2+\varepsilon}{3} + \dfrac{\varepsilon k_{\text{dis}_{yy}}}{k_f}\right)} \dfrac{4}{(\lambda L)^2}\left(1 - \dfrac{\tanh(\lambda L/2)}{(\lambda L/2)}\right)} \tag{45}$$

6 Conclusions

Upon introducing the effective porosity to account for the effects of tortuosity on the stagnant thermal conductivity, a thermal nonequilibrium model has been proposed for convection in a fluid saturated porous medium. Various analytical and empirical expressions for the stagnant thermal conductivities are compared against the experimental data available for the aluminum foam and air combination. Simple analytical expressions have been proposed to evaluate the thermal conductivities for the individual phases, which turn out to be significantly different from those based on simplified two equation models, used by most of previous investigators. Using the thermal nonequilibrium model, exact solutions are found, assuming a plug flow, for the two cases of thermally fully developed convective flows through a channel, namely, the case of isothermal hot and cold walls and the case of constant heat flux walls. The resulting temperature profiles across the channel for the case of metal foam and air combination reveals that the local thermal equilibrium assumption may hold for the case of isothermal walls, but, may fail for the case of constant heat flux walls.

Acknowledgment

This work was motivated by the remarks made by Professor N. Dukhan of University of Detroit Mercy to one of the authors (A. N.) during the Third International Conference on Porous Media and its Applications in Science, Engineering and Industry held in Montecatini, Italy, in June, 2010. The authors are grateful to Professor Dukhan for his useful suggestions made on this study.

Nomenclature

A = surface area (m^2)
A_{int} = interface between the fluid and solid (m^2)
c = specific heat (J/kgK)
c_p = specific heat at constant pressure (J/kgK)
d_m = mean pore diameter (m)
h_v = volumetric heat transfer coefficient (W/m^3K)
k = thermal conductivity (W/mK)
K = permeability (m^2)
L = channel height (m)
n_j = unit vector pointing outward from the fluid side to solid side (-)
Pr = Prandtl number (-)
q = heat flux (W/m^2)
T = temperature (K)
u_D = Darcian velocity (Uniform inlet velocity) (m/s)
u_i = velocity vector (m/s)
V = representative elementary volume (m^3)
x_i = Cartesian coordinates (m)
x, y, z = Cartesian coordinates (m)
ε = porosity (-)
ε^* = effective porosity (-)
ν = kinematic viscosity (m^2/s)
ρ = density (kg/m^2)

Special Symbols

$\tilde{\phi}$ = deviation from intrinsic average
$\langle\phi\rangle$ = Darician average
$\langle\phi\rangle^{f,s}$ = intrinsic average

Subscripts and Superscripts

dis = dispersion
f = fluid
s = solid
stag = stagnation
w = wall

References

[1] Nakayama, A., Kuwahara, F., Sugiyama, M., and Xu, G., 2001, "A Two-Energy Equation Model for Conduction and Convection in Porous Media," Int. J. Heat Mass Transfer, **44**(22), pp. 4375–4379.
[2] Yang, C., Liu, W., and Nakayama, A., 2009, "Forced Convective Heat Transfer Enhancement in a Tube With its Core Partially Filled With a Porous Medium," Open Transp. Phenom. J., **1**, pp. 1–6.
[3] Rees, D. A. S., and Pop, I., 2000, "Vertical Free Convective Boundary Layer, Flow in a Porous Medium Using a Thermal Nonequilibrium Model," J. Porous Media, **1**, pp. 31–44.
[4] Kuwahara, F., Shirota, M., and Nakayama, A., 2001, "A Numerical Study of Interfacial Convective Heat Transfer Coefficient in Two-Energy Equation Model for Convection in Porous Media," Int. J. Heat Mass Transfer, **44**, pp. 1153–1159.
[5] Quintard, M., 1998, "Modelling local non- equilibrium heat transfer in porous media," *Proceeding 11th International Heat Transfer Conference*, **1**, pp. 279–285.
[6] Quintard, M., and Whitaker, S., 1993, "One and Two Equation Models for Transient Diffusion Processes in Two-Phase Systems," Adv. Heat Transfer, **23**, pp. 369–465.
[7] Quintard, M., and Whitaker, S., 1995, "Local Thermal Equilibrium for Transient Heat Conduction: Theory and Comparison With Numerical Experiments," Int. J. Heat Mass Transfer, **38**, pp. 2779–2796.
[8] Minkowycz, W. J., Haji-Sheikh, A., and Vafai, K., 1999, "On Departure From Local Thermal Equilibrium in Porous Media Due to a Rapidly Changing Heat Source: The Sparrow Number," Int. J. Heat Mass Transfer, **42**, pp. 3373–3385.
[9] Kim, S. J., and Jang, S. P., 2002, "Effects of the Darcy Number, the Prandtl Number, and the Reynolds Number on Local Thermal Non-Equilibrium," Int. J. Heat Mass Transfer, **45**, pp. 3885–3896.
[10] Kiwan, S., and Al-Nimr, M. A., 2002, "Examination of the Thermal Equilibrium Assumption in Periodic Forced Convection in a Porous Channel," J. Porous Media, **5**, pp. 35–40.
[11] Al-Nimr, M. A., and Abu-Hijleh, B., 2002, "Validation of Thermal Equilibrium Assumption in Transient Forced Convection Flow in Porous Channel," Transp. Porous Media, **49**, pp. 127–138.
[12] Abu-Hijleh, B. A., Al-Nimr, M. A., and Hader, M. A., 2002, "Thermal Equilibrium in Transient Forced Convection Flow in Porous Channel," Transp. Porous Media, **49**, pp. 127–138.
[13] Khashan, S., Al-Amiri, A. M., and Al-Nimr, M. A., 2005, "Assessment of the Local Thermal Non-Equilibrium Condition in Developing Forced Convection Flows Through Fluid-Saturated Porous Tubes," Appl. Therm. Eng., **25**, pp. 1429–1445.
[14] Khashan, S., and Al-Nimr, M. A., 2005, "Validation of the Local Thermal Equilibrium Assumption in Forced Convection of Non-Newtonian Fluids Through Porous Channels," Transp. Porous Media, **61**, pp. 291–305.
[15] Haddad, O. M., Al-Nimr, M. A., and Al-Khateeb, A. N., 2004, "Validation of the Local Thermal Equilibrium Assumption in Natural Convection From a Vertical Plate Embedded in Porous Medium: Non-Darcian Model," Int. J. Heat Mass Transfer, **47**, pp. 2037–2042.
[16] Hsu, C. T., 2000, "Heat Conduction in Porous Media," *Handbook of Porous Media*, K. Vafai, ed., Marcel Dekker, New York, pp. 170–200.
[17] Hsu, C. T., Cheng, P., and Wong, K. W., 1995, "A Lumped Parameter Model for Stagnant Thermal Conductivity of Spatially Periodic Porous Media," ASME Trans. J. Heat Transfer, **117**, pp. 264–269.
[18] Kuznetsov, A. V., and Nield, D. A., 2010, "Effect of Local Thermal Non-Equilibrium on the Onset of Convection in a Porous Medium Layer Saturated by a Nanofluid," Transp. Porous Media, **83**, pp. 425–436.
[19] Kuznetsov, A. V., 1996, "A Perturbation Solution for a Nonthermal Equilibrium Fluid Flow Through a Three-Dimensional Sensible Heat Storage Packed Bed," J. Heat Transfer, **118**, pp. 508–510.
[20] Kuznetsov, A. V., 1997, "A Perturbation Solution for Heating a Rectangular Sensible Heat Storage Packed Bed With a Constant Temperature at the Walls," Int. J. Heat Mass Transfer, **40**, pp. 1001–1006.
[21] Yang, C., Ando, K., and Nakayama, A., 2011, "A Local Thermal Non-Equilibrium Analysis of Fully Developed Forced Convective Flow in a Tube Filled With a Porous Medium," Transp. Porous Media, (in press).

[22] Cheng, P., 1978, "Heat Transfer in Geothermal Systems," Adv. Heat Transfer, **14**, pp. 1–105.
[23] Nakayama, A., 1995, *PC-aided Numerical Heat Transfer and Convective Flow*, CRC, Boca Raton, FL, pp. 49–50, 103–115.
[24] Nakayama, A., Kuwahara, F., and Kodama, Y., 2006, "An Equation for Thermal Dispersion Flux Transport and Its Mathematical Modelling for Heat and Fluid Flow in a Porous Medium," J. Fluid Mech., **563**, pp. 81–96.
[25] Yang, C., and Nakayama, A., 2010, "A Synthesis of Tortuosity and Dispersion in Effective Thermal Conductivity of Porous Media," Int. J. Heat Mass Transfer, **53**(15–16), pp. 3222–3230.
[26] Paek, J. W., Kang, B. H., Kim, S. Y., and Hyun, J. M., 2000, "Effective Thermal Conductivity and Permeability of Aluminium Foam Materials," Int. J. Thermophys., **21**(2), pp. 453–464.
[27] Dul'nev, G. N., 1965, "Heat Transfer Through Solid Disperse Systems," J. Eng. Phys. Thermophys., **9**, pp. 275–279.
[28] Krishnan, S., Murthy, J. Y., and Garimella, S. V., 2006, "Direct Simulation of Transport in Open-Cell Metal Foam," J. Heat Transfer, **128**, pp. 793–799.
[29] Lemlich, R., 1978, "A Theory for the Limiting Conductivity of Polyhedral Foam at Low Density," J. Colloid Interface Sci., **64**, pp. 107–110.
[30] Calmidi, V. V., and Mahajan, R. L., 1999, "The Effective Thermal Conductivity of High Porosity Fibrous Metal Foams," ASME Trans. J. Heat Transfer, **121**, pp. 466–471.
[31] Calmidi, V. V., and Mahajan, R. L., 2000, "Forced Convection in High Porosity Metal Foams," ASME Trans. J. Heat Transfer, **122**, pp. 557–565.
[32] Bhattacharya, A., Calmidi, V. V., and Mahajan, R. L., 2002, "Thermophysical Properties of High Porosity Metal Foams," Int. J. Heat Mass Transfer, **45**, pp. 1017–1031.
[33] Singh, R., and Kasana, H. S., 2004, "Computational Aspects of Effective Thermal Conductivity of Highly Porous Metal Foams," Appl. Therm. Eng., **24**, pp. 1841–1849.
[34] Dukhan, N., Picon-Feliciano, R., and Alvarez-Hernandez, A. R., 2006, "Heat Transfer Analysis in Metal Foams With Low-Conductivity Fluids," J. Heat Transfer, **128**, pp. 784–792.
[35] Nakayama, A., Kuwahara, F., Umemoto, T., and Hayashi, T., 2002, "Heat and Fluid Flow Within an Anisotropic Porous Medium," ASME Trans. J. Heat Transfer, **124**, pp. 746–753.